Passive Fault Tolerant Control of a Double Inverted Pendulum

A Case Study

Stoustrup, Jakob; Niemann, H.

Published in:
Control Engineering Practice

DOI (link to publication from Publisher):
10.1016/j.conengprac.2004.11.002

Publication date:
2005

Document Version
Early version, also known as pre-print

Available online at www.sciencedirect.com
SCIENCE DIRECT®
Control Engineering Practice 13 (2005) 1047–1059
CONTROL ENGINEERING PRACTICE
www.elsevier.com/locate/conengprac

Passive fault tolerant control of a double inverted pendulum—a case study

Henrik Niemann[a,*], Jakob Stoustrup[b]

[a]Technical University of Denmark, Ørsted-DTU, Automation, Building 326, DK-2800 Lyngby, Denmark
[b]Department of Control Engineering, Aalborg University, Fr. Bajers Vej 7C, DK-9220 Aalborg, Denmark

Received 28 October 2003; accepted 4 November 2004
Available online 25 December 2004

Abstract

A passive fault tolerant control scheme is suggested, in which a nominal controller is augmented with an additional block, which guarantees stability and performance after the occurrence of a fault. The method is based on the YJBK parameterization, which requires the nominal controller to be implemented in observer based form. The proposed method is applied to a double inverted pendulum system, for which an $\mathscr{H}_\infty$ controller has been designed and verified in a lab setup. In this case study, the fault is a degradation of the tacho loop.

Keywords: $\mathscr{H}_\infty$ controller design; YJBK parameterization; Fault tolerant control; Observer based controller implementation; Simulation

1. Introduction

The pendulum system is one of the classical examples used in connection with feedback control. The single inverted single pendulum is a standard example in many text books dealing with classical as well as modern control. The reason is that the system is quite simple, nonlinear and unstable. In classical control courses, the single inverted pendulum system has among other things been used to show that the system cannot be stabilized by using just a proportional (P) controller. In spite of the fact that the system is unstable, the design of stabilizing controllers for the system can be done reasonable easy. However, this is not the case when considering the quite more complicated double inverted pendulum system. It is much more challenging to design/tune stabilizing controllers for this system. Therefore, more advanced controller architectures and advanced design methods should be applied. Previous work has involved various types of model based controllers designed by using e.g. $\mathscr{H}_2$ based methods, $\mathscr{H}_\infty$ based methods and μ based methods. An investigation of different robust controllers for the double inverted pendulum system has been described in Niemann and Poulsen (2003, 2005) and Poulsen (2001).

In this paper, the double inverted pendulum system will be applied in connection with design of a fault tolerant controllers (FTC). The area of FTC has been an increasing research area for the past 5–10 years, see Blanke, Frei, Kraus, Patton, and Staroswiecki (2000); Blanke, Staroswiecki, and Wu (2001); Wu and Chen (1996); Wu, Zhou, and Salomon (2000) and the references in these. The reason is the increasing use of increasingly complex control systems. This will in general require a supervision level on top of the control level to handle faulty situations in a systematic way. One part of this supervision is to use FTC. The key idea of using FTC is to keep the closed loop system stable while possibly accepting a reduced performance when (critical) faults occur in the system. This can be done either

*Corresponding author. Tel.: +45 45 25 35 59; fax: +45 45 88 12 95.
E-mail addresses: hhn@oersted.dtu.dk (H. Niemann), jakob@control.aau.dk (J. Stoustrup).
URLS: http://www.oersted.dtu.dk/staff/all/hhn/, http://www.control.aau.dk/~jakob/.

0967-0661/$ - see front matter © 2004 Elsevier Ltd. All rights reserved.
doi:10.1016/j.conengprac.2004.11.002

by a reconfiguration of the feedback controller, Blanke et al. (2000), or by using a passive approach, where the fault tolerance is included in the controller architecture, see e.g. Niemann and Stoustrup (2002); Stoustrup and Niemann (2001). The general (active) FTC architecture was derived in Zhou and Ren (2001) and independently in Stoustrup and Niemann (2001) for continuous-time systems. A description can be found in Niemann and Stoustrup (2004) for sampled-data systems. The passive FTC concept will be applied in this paper. The advantages with that concept is that no time delay will be included in the controller due to detection of faults and a following reconfiguration of the controller. An active FTC control is virtually impossible to implement for an unstable system like the one considered in this paper for which the time window, where the system stays stabilizable is too small to obtain a reliable fault detection signal. The disadvantage with the passive concept is that it can only handle a single fault or a few faults.

The general FTC architecture considered consists of two parts, a fault detection and isolation (FDI) part and a controller reconfiguration (CR) part. Both parts are based on the Youla–Jabr–Bongiorno–Kucera (YJBK) parameterization of all stabilizing controllers, see Youla, Bongiorno, and Jabr(1976a,b). The nominal feedback controller for the fault free system is applied as the basis for the YJBK parameterization. The passive FTC architecture consists only of the controller reconfiguration part of the general FTC architecture. In this passive approach, the YJBK parameter is applied both in connection with the feedback controller for the fault free system to optimize the closed loop performance and in the faulty case for stabilizing the closed-loop system, i.e. there will be no switching in the controller. Further, this will result in a multi objective design problem for the design of the YJBK parameter (controller). The parameter must be optimized with respect to both the nominal case as well as the faulty case.

Passive fault tolerant control has strong relations to the part of robust control theory, which addresses the problem of designing one compensator with the potential of controlling several systems. The main difference is that passive FTC emphasises one system in particular, i.e. the nominal system. The control of the faulty situations will often be based on a 'limb home' strategy, but in any case, it should be possible to control the detuning of the control of the nominal controller in favor of the faulty situations. The proposed approach is very explicit in this respect, in the sense that it embarks from a nominal controller and introduces fault tolerance by virtue of an explicit detuning parameter, which is really a handle that can be turned to control the trade-off between nominal and faulty situations.

In this case study example, the FTC controllers are designed with respect to a single fault in the tacho loop in the motor, i.e. a broken tacho loop or a major reduction of the tacho gain. A broken tacho loop or a major reduction of the tacho gain will result in an unstable closed loop system if no corrective measures are taken. Due to the limitations in the system, the fault tolerant part of the controller needs to be active immediately after the tacho fault appear. Even a minor time delay between the fault appears and the FTC controller that becomes active cannot be accepted in this case.

The rest of this paper is organized as follows. In Section 2, the double inverted pendulum system is shortly described, including a design of controllers for the fault free system. The FTC architecture is shortly introduced and the FTC design with respect to a fault at the tacho loop is described in Section 3. Section 4 includes a simulation of the passive FTC for the double inverted pendulum system followed by a conclusion in Section 5.

2. Model of a double inverted pendulum

In the following, a short description of the double inverted pendulum system is given. Both the nominal as well as the laboratory model are considered. A more detailed description can be found in Niemann and Poulsen (2003, 2005); Poulsen (2001).

The double inverted pendulum consist of a cart placed on a track, and two aluminum arms connected to each other. These are constrained to rotate within a single plane. The axis of the rotation is perpendicular to the direction of the motion of the cart. The cart is attached to the bottom of the pendulum, and moving along a linear low friction track. The cart is moved by an exerting force by a servo motor system. A nonlinear model for the complete system can be derived by using Newton's second and third laws on every part of the system. The nonlinear model of the system is included in Appendix A.

Based on the nonlinear model given in Appendix A, a linear model can be derived by a linearization of the nonlinear model around the working point. The linear model Σ for the complete system can be described by the following state space description

$$\Sigma: \begin{cases} \dot{x} = Ax + B_w w + B_u u, \\ z = C_z x + D_{zw} w + D_{zu} u, \\ y = C_y x + D_{yw} w + D_{yu} u, \end{cases} \tag{2.1}$$

or as transfer functions

$$\Sigma: \begin{cases} z = G_{zw} w + G_{zu} u, \\ y = G_{yw} w + G_{yu} u, \end{cases} \tag{2.2}$$

where x is the state, w is the exogenous inputs, u is the control input and (the output voltage U), y is the measurement output. z is an external output vector, see

below. The linear model is of order seven with the following states:

$$x = [\theta_1\ \dot{\theta}_1\ \theta_2\ \dot{\theta}_2\ x_c\ \dot{x}_c\ i]^{\mathrm{T}}, \tag{2.3}$$

where θ_1 is the angle between vertical and the lower arm, $\dot{\theta}_1$ is the angular velocity related to θ_1, θ_2 is the angle between vertical and the upper arm, $\dot{\theta}_2$ is the angular velocity related to θ_2, x_c is the cart position, $\dot{x}_c$ is the velocity of the cart and i is the motor current.

The exogenous input vector are given by

$$w = [r_c\ M_{d_1}\ M_{d_2}\ n_1\ n_3\ M_{dm}\ n_x]^{\mathrm{T}}, \tag{2.4}$$

where r_c is the cart position reference, M_{d_1} and M_{d_2} are the torque disturbance on the joint on the lower arm and on the upper arm, respectively, n_1 and n_3 are noise signal in measuring θ_1 and $\theta_3 = \theta_1 - \theta_2$, respectively, M_{dm} is the torque disturbance on the motor, and n_x is the noise signal in the measuring of the cart position x_c.

The measurement vector y is given by

$$y = [e_c\ \theta_1\ \theta_3]^{\mathrm{T}}, \tag{2.5}$$

where e_c is the cart position error, i.e. $e_c = r_c - x_c$.

The state space matrices in (2.1) can be found in Appendix B.

2.1. Nominal controller design

A nominal feedback controller is designed by using the standard $\mathscr{H}_\infty$ design approach, Skogestad and Postlethwaite (1996); Zhou, Doyle, and Glover (1995). The system setup given by (2.1) is extended by a multiplicative output uncertainty described by

$$G_p = (I + W_o \Delta_o)G, \tag{2.6}$$

where the perturbation matrix Δ_o satisfies $\|\Delta_o\|_\infty \leqslant 1$ as in Skogestad and Postlethwaite (1996) and W_o is a weight that indicates a potential relative error as a function of frequency. The multiplicative perturbation represent a lumping of parameter variations and uncertain dynamics into a single perturbation block. The performance for the system is described by including an external output vector z given by

$$z = [e_c\ \theta_1\ \theta_2\ u\ i]^{\mathrm{T}}, \tag{2.7}$$

where u is the control signal and i is the current in the motor. The complete design setup is shown in Fig. 1. W_p is a weighting matrix for the performance specification.

Four different controller designs have been described in Niemann and Poulsen (2003, 2005), three controllers designed by using the standard $\mathscr{H}_\infty$ optimization and one controller by using μ synthesis. In this paper, we will apply an $\mathscr{H}_\infty$ optimized controller obtained by using the following weight matrices:

$$W_o = \mathrm{diag}(W_{o1} W_{o2}),$$
$$W_P = \mathrm{diag}(W_e, W_{\theta_1}, W_{\theta_2}, W_U, W_i), \tag{2.8}$$

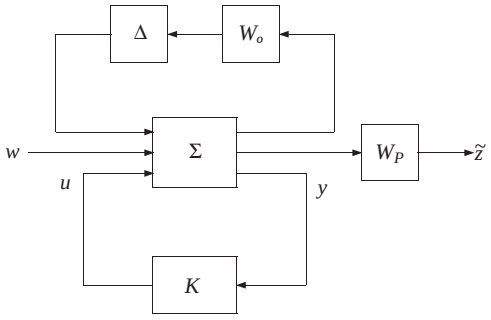

Fig. 1. The complete system setup for design of robust feedback controllers.

where

$$W_{o1} = W_{o2} = 0, \quad W_e = \frac{25}{50s + 1},$$

$$W_{\theta_1} = \frac{50}{s + 10}, \quad W_{\theta_2} = \frac{45}{s + 10},$$

$$W_U = 0.1\frac{s + 100}{0.01s + 100}, \quad W_i = 0.01,$$

i.e. a nominal controller design. The final controller is of order 11, but has been reduced to order seven, the same order as the nominal plant, see Niemann and Poulsen (2003, 2005). A simulation of the applied nominal controller is shown in Fig. 2, and in Fig. 3, the $\mathscr{H}_\infty$ controller is applied to the laboratory system.

3. Design of a fault tolerant controller

The design of a passive FTC for the double inverted pendulum system is based on the results described in Niemann and Stoustrup (2002, 2004).

3.1. A general FTC architecture

First, the general FTC architecture proposed in Niemann and Stoustrup (2002, 2004) is shortly introduced. The architecture is based on the YJBK parameterization. The YJBK parameterization was derived in Youla et al.(1976a,b) and independently in Kucera (1975).

Let a coprime factorization of the system $G_{yu}(s)$ from (2.2) and a stabilizing controller $K(s)$ be given by

$$G_{yu} = NM^{-1} = \tilde{M}^{-1}\tilde{N}, \quad N, M, \tilde{N}, \tilde{M} \in \mathscr{RH}_\infty,$$
$$K = UV^{-1} = \tilde{V}^{-1}\tilde{U}, \quad U, V, \tilde{U}, \tilde{V} \in \mathscr{RH}_\infty, \tag{3.1}$$

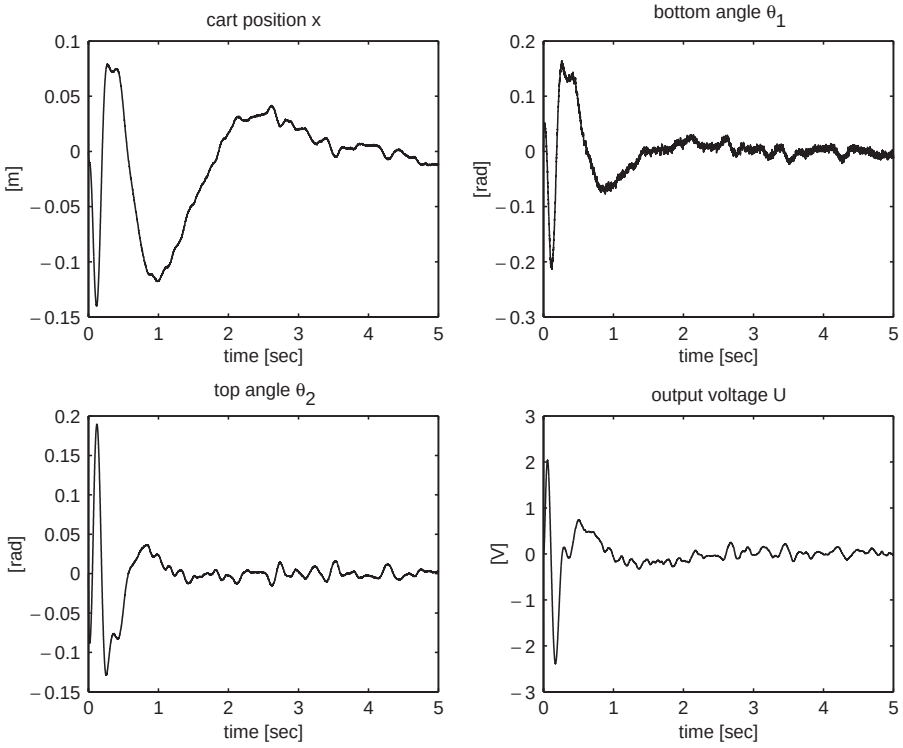

Fig. 2. Simulation of the nonlinear system with an $\mathscr{H}_\infty$ controller. The initial conditions are: $\theta_1 = 0.05$ rad and $\theta_2 = -0.04$ rad, similar to what would happen for the lab. model.

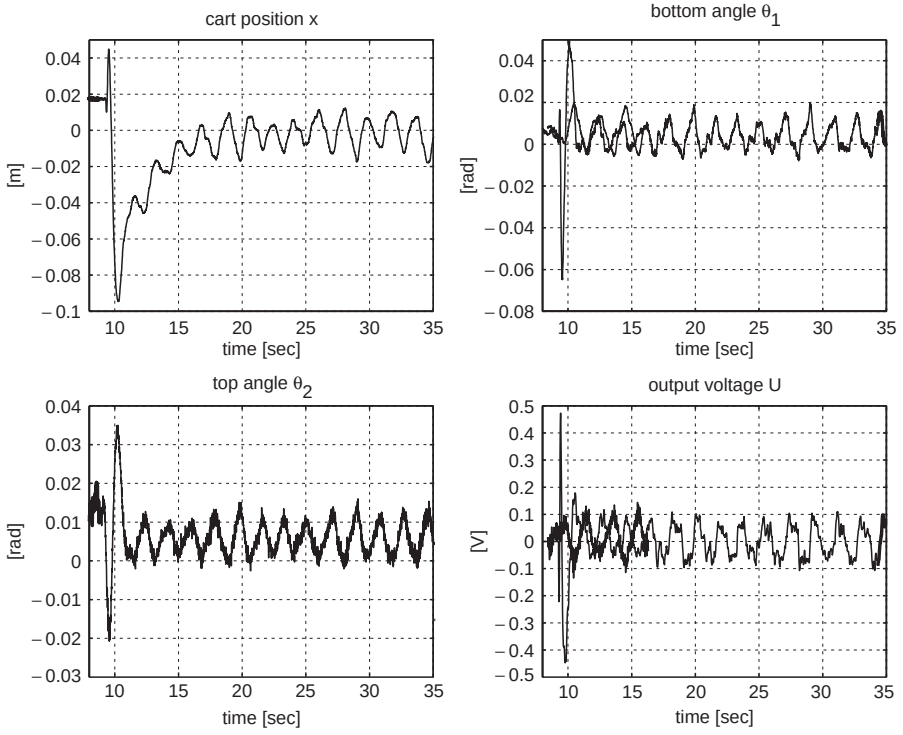

Fig. 3. Sampled data from laboratory model, running with an $\mathscr{H}_\infty$ controller.

where the eight matrices in (3.1) must satisfy the double Bezout equation given by, see Zhou et al. (1995):

$$\begin{pmatrix} I & 0 \\ 0 & I \end{pmatrix} = \begin{pmatrix} \tilde{V} & -\tilde{U} \\ -\tilde{N} & \tilde{M} \end{pmatrix} \begin{pmatrix} M & U \\ N & V \end{pmatrix} = \begin{pmatrix} M & U \\ N & V \end{pmatrix} \begin{pmatrix} \tilde{V} & -\tilde{U} \\ -\tilde{N} & \tilde{M} \end{pmatrix}. \tag{3.2}$$

Based on the above coprime factorization of the system $G_{yu}(s)$ and the controller $K(s)$, we can give a parameterization of all controllers that stabilize the system in terms of a stable parameter $Q(s)$, i.e. all stabilizing controllers are given by Tay, Mareels, and Moore (1997):

$$K(Q) = U(Q)V(Q)^{-1}, \tag{3.3}$$

where

$$U(Q) = U + MQ, \quad V(Q) = V + NQ, \quad Q \in \mathscr{RH}_\infty,$$

or by using a left factored form

$$K(Q) = \tilde{V}(Q)^{-1}\tilde{U}(Q), \tag{3.4}$$

where

$$\tilde{U}(Q) = \tilde{U} + Q\tilde{M}, \quad \tilde{V}(Q) = \tilde{V} + Q\tilde{N}, \quad Q \in \mathscr{RH}_\infty.$$

Using the Bezout equation, the controller given either by (3.3) or by (3.4) can be realized as an LFT in the parameter Q,

$$K(Q) = \mathscr{F}_l(J_K, Q), \tag{3.5}$$

where J_K is given by

$$J_K = \begin{pmatrix} UV^{-1} & \tilde{V}^{-1} \\ V^{-1} & -V^{-1}N \end{pmatrix} = \begin{pmatrix} \tilde{V}^{-1}\tilde{U} & \tilde{V}^{-1} \\ V^{-1} & -V^{-1}N \end{pmatrix}. \tag{3.6}$$

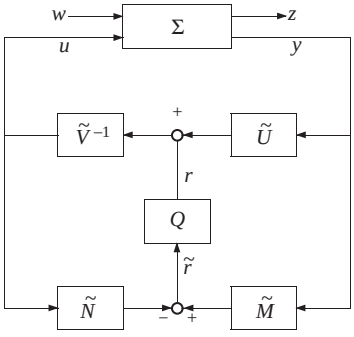

Fig. 4. Controller structure with parameterization.

Reorganizing the controller $K(Q)$ given by (3.5) results in the closed loop system depicted in Fig. 4, Tay et al. (1997).

The main observation which shall be exploited in the solution to the fault tolerant control problem, is the following relatively simple expression for the transfer function from the external input w to the external output z terms of the parameter Q:

$$\begin{aligned} z &= (G_{ed} + G_{eu}K(Q)(I - G_{yu}K(Q))^{-1}G_{yd})w \\ &= (G_{ed} + G_{eu}U\tilde{M}G_{yd} + G_{eu}MQ\tilde{M}G_{yd})w, \end{aligned}$$

where (3.2) has been exploited. Note, that the transfer function relating w and z is affine in Q.

The FTC architecture is based directly on the YJBK parameterization shown in Fig. 4. Using this architecture, the Q parameter will be the CR part of the controller. This means that the CR part of the feedback controller is a modification of the existing controller. Thus, a controller change when a fault appears in the system is not a complete shift to another controller, but only a modification of the existing controller by adding a correction signal in the nominal controller, the r signal in Fig. 4. However, it should be pointed out that it is possible to modify the controller arbitrarily by designing the YJBK parameter Q, see e.g. Niemann, Stoustrup, and Abrahamsen (2004); Tay et al. (1997).

Another important thing is that the architecture also includes a parameterization of all residual generators. All residual signals can be described by, Frank and Ding (1994); Gertler (1998)

$$r = Q_{FDI}\tilde{r} = Q_{FDI}(\tilde{M}y - \tilde{N}u), \tag{3.7}$$

where the stable Q_{FDI} is called the parameterization matrix for the residual generator. The design of Q_{FDI} must be done with respect to optimize the residual vector r. Based on this optimized residual vector, fault detection/fault isolation can be develop by using e.g. a CUSUM or a GLR test. This means that it is possible to combine both fault diagnosis and fault tolerant control in the same architecture without any problems. A block diagram for this combined FDI and FTC architecture based on the YJBK parameterization is shown in Fig. 5 for three potential multiplicative faults—the generalization to any number of faults should be obvious.

3.2. Observer based controllers

The implementation of the YJBK parameterized controller utilizes an observer based feedback controller. The YJBK parameterized controller is given by (3.5)

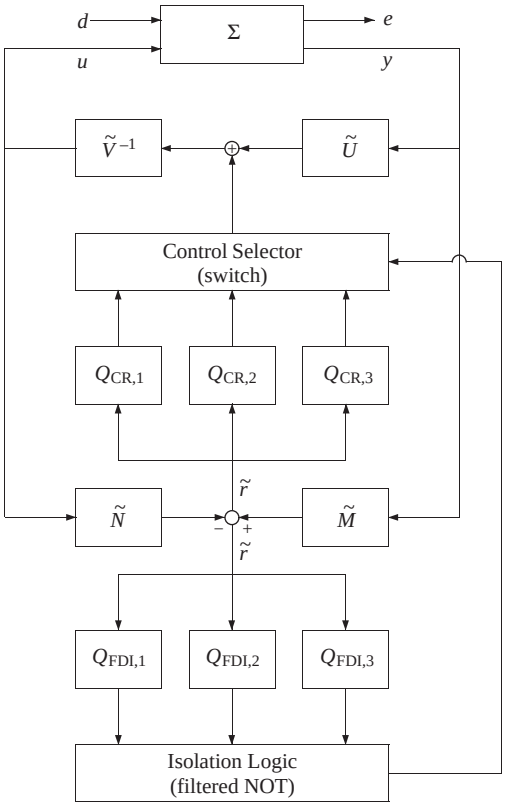

Fig. 5. Fault tolerant scheme with three potential multiplicative faults. The residual signal is used both for isolation and for feedforward in the fault handling.

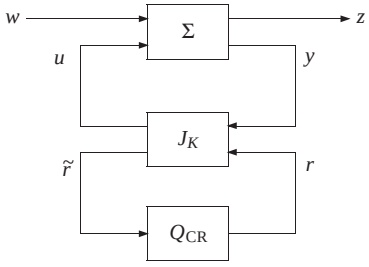

Fig. 6. The architecture setup for the passive FTC.

with J_K is given by

$$J_K = \left(\begin{array}{c|cc} A + B_u F + LC_y & -L & B_u \\ \hline F & 0 & I \\ -C_y & I & 0 \end{array}\right), \tag{3.8}$$

where F is a stabilizing state feedback gain such that $A + B_u F$ is stable and L is a stabilizing observer gain such that $A + LC_y$ is stable. The passive FTC controller architecture is shown in Fig. 6.

The final seventh order controller (designed by using the $\mathscr{H}_\infty$. design method followed by a model reduction) is transformed into an observer based controller by using the method described in Alazard and Apkarian (1999, 2002). Using this method, we get the state feedback gain F and the observer gain L for the controller given in Appendix C.

3.3. FTC design setup

The FTC controller is designed with respect to a broken or damaged tacho loop. The tacho fault is described by using a multiplicative (parameter) fault model given by

$$\Sigma_M : \begin{cases} z_\theta = G_{z_\theta w_\theta} w_\theta + G_{z_\theta w} w + G_{z_\theta u} u, \\ z = G_{z w_\theta} w_\theta + G_{z w} w + G_{z u} u, \\ y = G_{y w_\theta} w_\theta + G_{y w} w + G_{y u} u, \end{cases} \tag{3.9}$$

where $w_\theta \in \mathbb{R}^{k_w}$ and $z_\theta \in \mathbb{R}^{k_z}$ are the external input and output vectors. The connection between the external output and the external input is given by

$$w_\theta = \theta z_\theta,$$

where θ represent the multiplicative (parameter) faults in the system. Note that the above description is also applied in connection with description of systems including model uncertainties, see e.g. Zhou et al. (1995). In this case, θ is a scalar parameter, where $\theta = 0$ describes the fault free system and $\theta = 1$ describes the system with a broken tacho loop.

The design of Q_{CR}, the passive FTC, will be based on an optimization of the performance of the fault free closed loop system and at the same time a stabilization of the faulty system. This results in a multi objective design of Q_{CR}. Based on the system given in (3.9), the performance design problem for the fault free system is then given by Stoustrup and Niemann (2001) and Tay et al. (1997):

$$\|T_{zw}\|_\infty = \|T_1 + T_2 Q_{CR} T_3\|_\infty < \gamma, \quad Q_{CR} \in \mathscr{RH}_\infty \tag{3.10}$$

for a specified $\gamma > 0$, where T_1, T_2 and T_3 are functions of the open loop transfer functions in (3.9) for $\theta = 0$. When a fault occurs in the system, in this case a broken tacho loop, the closed loop transfer function will no longer be an affine function of the Q_{CR} controller as in (3.10). A broken tacho loop or a reduction of the tacho gain results in an unstable closed loop system. The design problem for the faulty system is then a stabilization problem. Let $\tilde{T}_4$ be the transfer function from r to $\tilde{r}$ for $\theta \in]0, 1]$, see Fig. 6. The FTC design problem is then as follows, Niemann and Stoustrup (2002):

$$(I - \tilde{T}_4 Q_{CR})^{-1} \in \mathscr{RH}_\infty. \tag{3.11}$$

Note that $\tilde{T}_4$ is also known as the dual YJBK parameter S, see Niemann and Stoustrup (2002). However, it is also possible to include performance requirements in the design of Q_{CR} controller. This can be done by optimizing Q_{CR} with respect to the external inputs/outputs, i.e.

$$\|\tilde{T}_{zw}(Q_{CR})\|_\infty < \gamma, \; Q_{CR} \in \mathscr{RH}_\infty, \tag{3.12}$$

where

$$\tilde{T}_{zw}(Q_{CR}) = \tilde{T}_1 + \tilde{T}_2 Q_{CR}(I - \tilde{T}_4 Q_{CR})^{-1}\tilde{T}_3.$$

Based on this, it is possible to formulate a number of passive FTC design problems. In the first design problem, the main passive fault tolerant control design problem is given. Here, the stability conditions for the nominal and the faulty system is the main design condition.

Problem 1. The passive FTC design problem is defined as the problem of designing Q_{CR}, $Q_{CR} \in \mathscr{RH}_\infty$ such that

$$(I - \tilde{T}_4 Q_{CR})^{-1} \in \mathscr{RH}_\infty.$$

In the next design problem, the CR part of the controller is optimized with respect to the performance of the nominal closed loop system together with the stability condition.

Problem 2. Let $\gamma > 0$ be given. The passive FTC design problem with respect to an $\mathscr{H}_\infty$ optimization of the nominal performance is to design Q_{CR}, $Q_{CR} \in \mathscr{RH}_\infty$ such that

$$\|T_1 + T_2 Q_{CR} T_3\|_\infty < \gamma,$$

$$(I - \tilde{T}_4 Q_{CR})^{-1} \in \mathscr{RH}_\infty.$$

In the last passive FTC design problem, the CR part of the controller is designed with respect to both the stability of the faulty system and with respect to optimize the performance of both the nominal system and the faulty system.

Problem 3. Let $\gamma_2 \geqslant \gamma_1 > 0$ be given. The passive FTC design problem with respect to an $\mathscr{H}_\infty$ optimization of the nominal performance and the performance in the faulty system is to design Q_{CR}, $Q_{CR} \in \mathscr{RH}_\infty$ such that

$$\|T_1 + T_2 Q_{CR} T_3\|_\infty < \gamma_1,$$

$$\|\tilde{T}_1 + \tilde{T}_2 Q_{CR}(I - \tilde{T}_4 Q_{CR})^{-1}\tilde{T}_3\|_\infty < \gamma_2.$$

An $\mathscr{H}_\infty$ norm has been applied in Problems 2 and 3. However, it is also possible to use the $\mathscr{H}_2$ norm instead.

The design of Q_{CR} for the double inverted pendulum system has been derived by using a slightly modified version of Problem 3. Problem 3 is a multiobjective design problem. Instead, the design of Q_{CR} has been done with respect to optimizing the performance of the faulty system followed by a validation of the performance for the nominal closed loop system. An $\mathscr{H}_\infty$ design method has been used for the design of Q_{CR}. Using this method for the design of Q_{CR} given that it is not possible to design a stable Q_{CR} with a complete broken tacho loop. Instead, a reduction of the tacho gain with 70% is considered for the passive FTC design.

The final controller Q_{CR} is of order 18. The controller order has not been reduced in the simulation. However, it is possible to reduce it to a much lower order without any problems. The magnitude of the nominal $\mathscr{H}_\infty$ controller K_{nom} as well as for the passive FTC controller

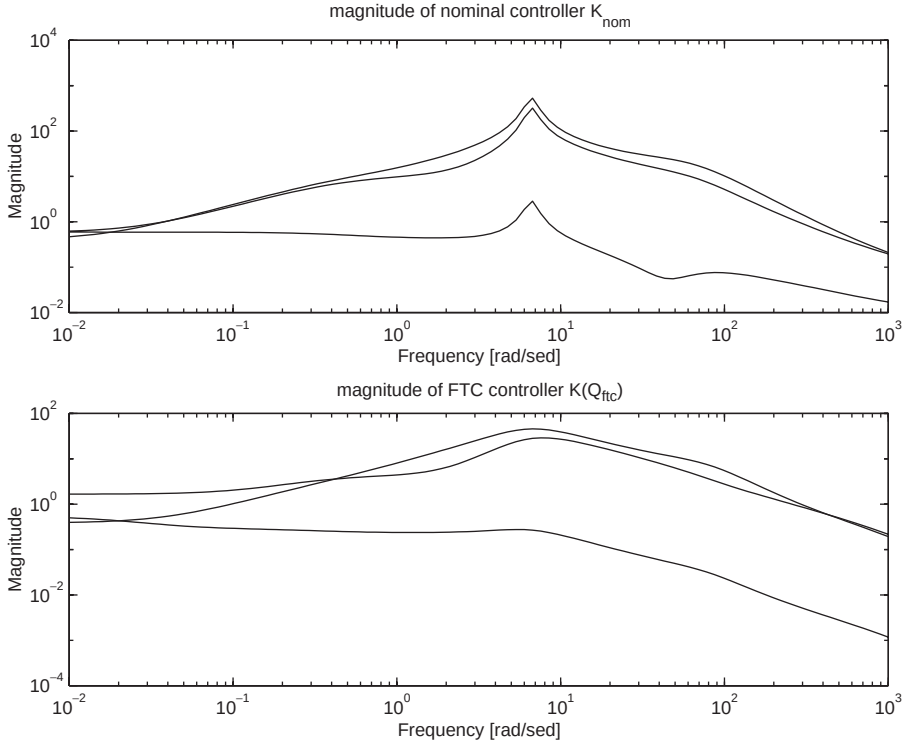

Fig. 7. The magnitude of the nominal controller K_{nom} and of the passive FTC controller $K(Q_{CR})$.

$K(Q_{CR})$ is shown in Fig. 7. It is clear that the gain of the passive FTC controller has been reduced compared with the nominal controller. As a consequence of this, a reduction in the performance of the nominal closed loop system is expected.

Simulations of the faulty system with the FTC are shown in the following section.

4. Simulation results

A number of simulations with the faulty system are shown in this section. The passive FTC system is simulated under the following conditions: At $t = 0.5$ s, the Q_{CR} part is included in the closed loop system. At $t = 2.0$ s, the gain of the tacho loop is reduced with 70%. Further, a Gaussian disturbance has been included at the two angles, θ_1 and θ_2, and at the cart position x_c. The results of the simulations are shown in Figs. 8–11.

In Fig. 8, the faulty system is simulated with the nominal controller. It is clear that the faulty closed loop system is unstable.

The performance of the fault free system when the passive FTC controller $K(Q_{CR})$ is applied can be seen from Fig. 9. A reduction of the performance of the closed loop system is the result of using the passive FTC controller compared with the closed loop system based on K_{nom}—compare with the simulation in Fig. 2. This is also in line with results shown in Fig. 7. In Fig. 10, the faulty system has been simulated when the passive FTC controller has been applied. As it can be seen, the closed loop system is now stable. It is also clear that the performance of the closed loop has been reduced compared with the fault free system, see Fig. 2. In Fig. 11, the two control signals (u and y_q) are shown. It is quite clear that the Q_{CR} part of the controller is very active after the fault has appeared in the system. This part of the controller needs to take over for the reduced tacho feedback loop.

5. Conclusion

An architecture for passive FTC has been applied on a double inverted pendulum system. The passive FTC architecture is based on the YJBK parameterization of all stabilizing controllers. Three passive FTC problems has been formulated for the design of Q_{CR} for the pendulum system. The design of Q_{CR} with respect to a fault in the tacho loop has been derived by using an $\mathscr{H}_\infty$ optimization method. The final FTC controller has been simulated on the faulty pendulum system.

The introduction of a passive FTC controller in the loop has reduced the performance of the nominal fault free system. The design of the CR part of the feedback controller is a trade-off between the performance of the nominal fault free pendulum system and the performance of the faulty pendulum system. In this case study,

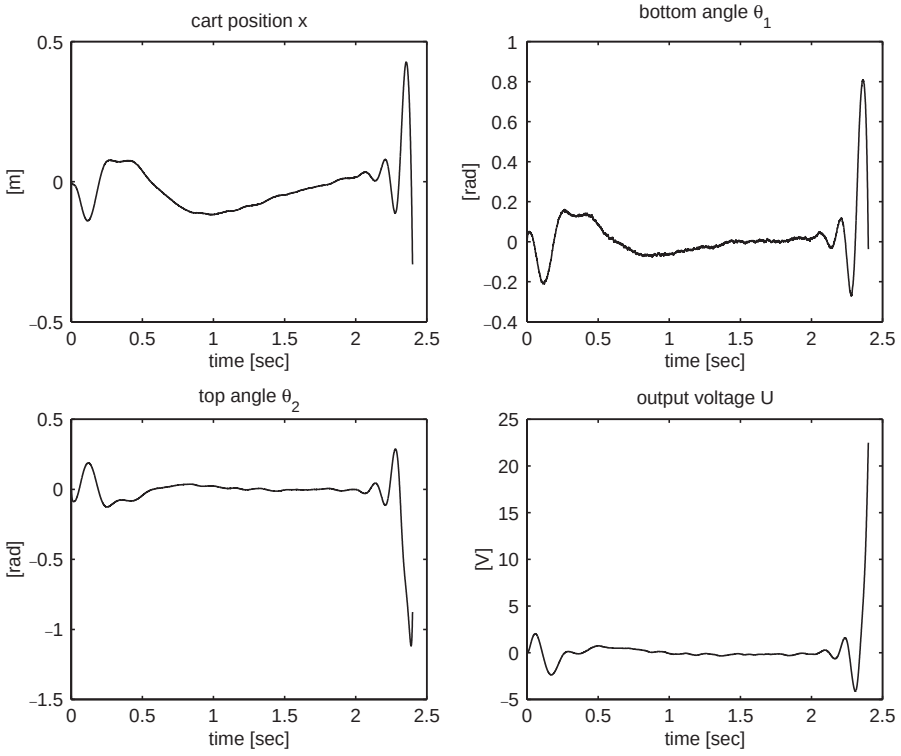

Fig. 8. Simulation of the nonlinear system with the $\mathscr{H}_\infty$ controller. The initial conditions are: $\theta_1 = 0.05$ rad and $\theta_2 = -0.04$ rad. The gain in the tacho loop is reduced with 70% at $t = 2$ s.

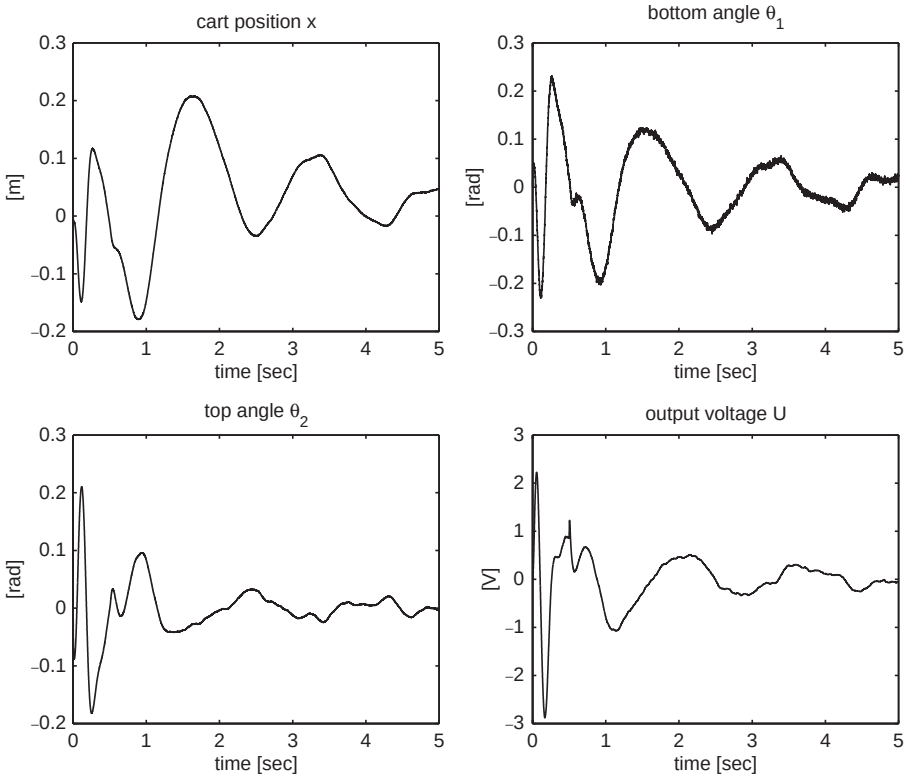

Fig. 9. Simulation of the fault free nonlinear system with the passive FTC controller $K(Q_{CR})$. The initial conditions are: $\theta_1 = 0.05$ rad and $\theta_2 = -0.04$ rad. The Q_{CR} controller is included in the control loop after $t = 0.5$ s.

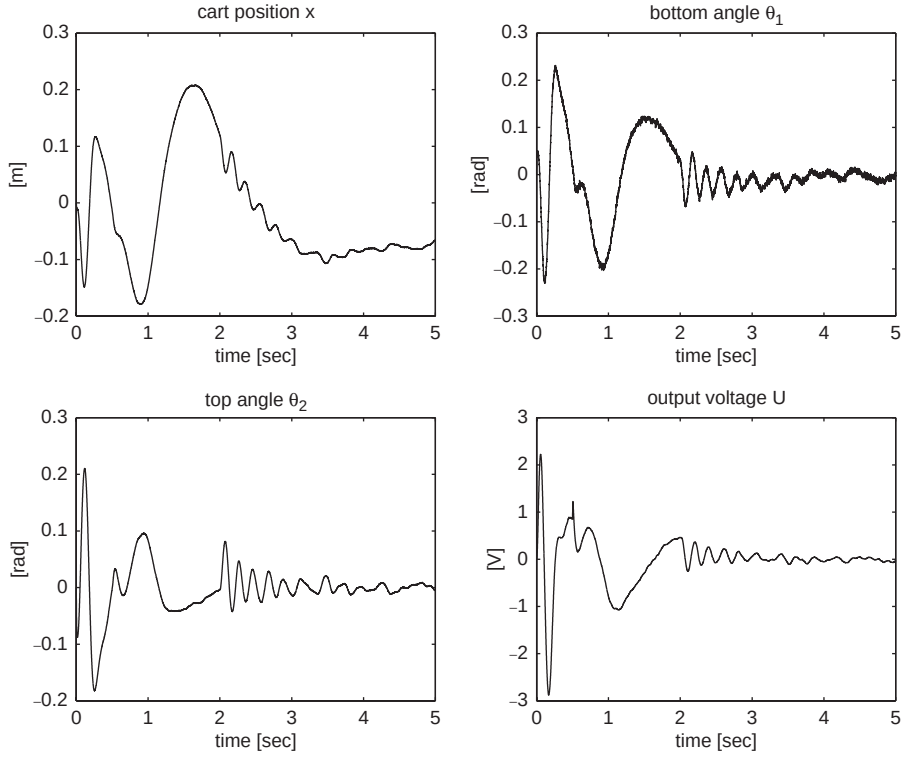

Fig. 10. Simulation of the nonlinear system with the passive FTC controller $K(Q_{CR})$. The initial conditions are: $\theta_1 = 0.05$ rad and $\theta_2 = -0.04$ rad. The Q_{CR} controller is included in the control loop after $t = 0.5$ s. The gain in the tacho loop is reduced with 70% at $t = 2$ s.

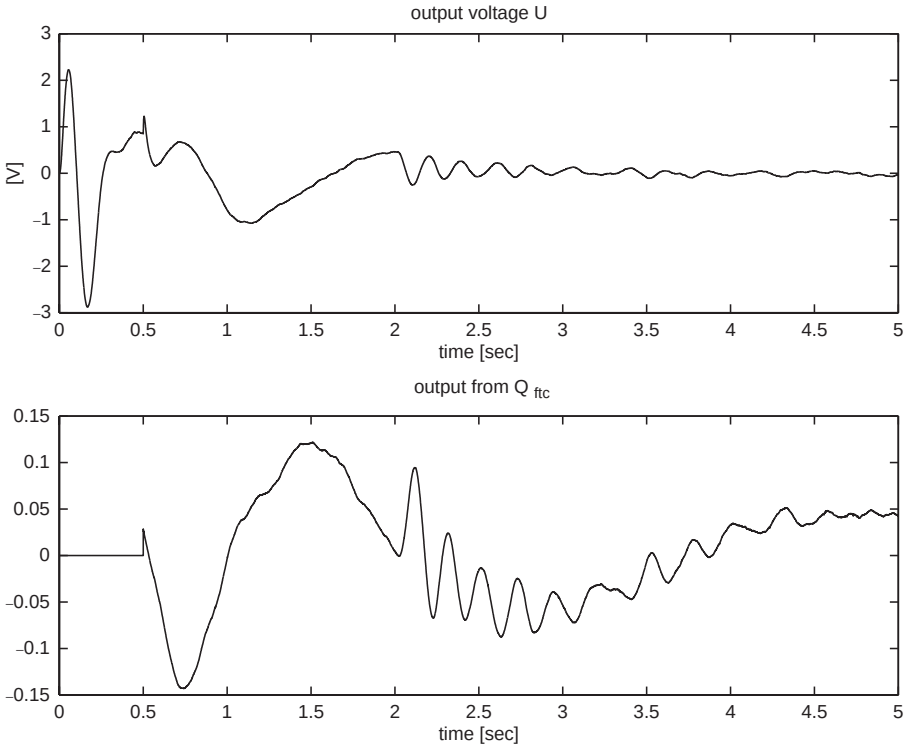

Fig. 11. The control signal from the controller $K(Q)$ and from the Q_{CR} controller for the simulation of the nonlinear system with the $\mathscr{H}_\infty$ controller. The initial conditions are: $\theta_1 = 0.05$ rad and $\theta_2 = -0.04$ rad. The Q_{CR} controller is included in the control loop after $t = 0.5$ s. The gain in the tacho loop is reduced with 70% at $t = 2$ s.

the selected passive FTC controller reduces the performance of the fault free system with 25–50% compared to the nominal controller. The performance of the faulty pendulum system is comparable with the performance of the nominal system.

The pendulum system example also shows one of the disadvantages by using this passive FTC architecture. Since the FTC architecture is based on the YJBK parameterization, the YJBK parameter needs to satisfy the stability condition from the YJBK parameterization, i.e. Q_{CR} must be open-loop stable. In this example, it was not possible to design an open-loop stable Q_{CR} controller for the setup by using the standard regular $\mathscr{H}_2$ or the standard regular $\mathscr{H}_\infty$ design method for a completely broken tacho loop. This does not necessarily mean that there does not exist an open-loop stable Q_{CR} for the pendulum system with a complete broken tacho loop—just that it needs a dedicated numerical algorithm. If instead the active FTC architecture had been applied, the open loop stability condition for Q_{CR} would no longer be required. The reason is that Q_{CR} would only appear in a closed loop feedback system.

Appendix A. The nonlinear model

The double inverted pendulum consists of a cart placed on a rail, and two aluminum arms connected to each other. These are constrained to rotate within a single plane. The axis of the rotation is perpendicular to the direction of the motion of the cart. The cart is attached to the bottom of the pendulum, and moving along a linear low friction rail. The cart is moved by an exerting force by a servo motor system. A principal structure of the pendulum system is shown in Fig. 12, where the forces acting on the system has been included.

The system consists of a standard DC servo system and the pendulum system. These two systems are described in the following.

A.1. Servo system

The servo DC system is a standard servo system including a tacho feedback loop. The equations for the servo system are given.

The torque:

$$I_m\ddot{\theta}_m = K_t i - K_{dm}M_{dm} - \frac{r_{c3}}{N}F_{cm},$$

where the inertia I_m seen from the motor axis is given by

$$I_m = I_{mr} + \frac{1}{2}\left[M_{c1}r_{c1}^2 + \frac{1}{N}\left(M_{c2}r_{c2}^2 + 2M_{c3}r_{c3}^2 + 2M_{axle}r_{axle}^2\right)\right].$$

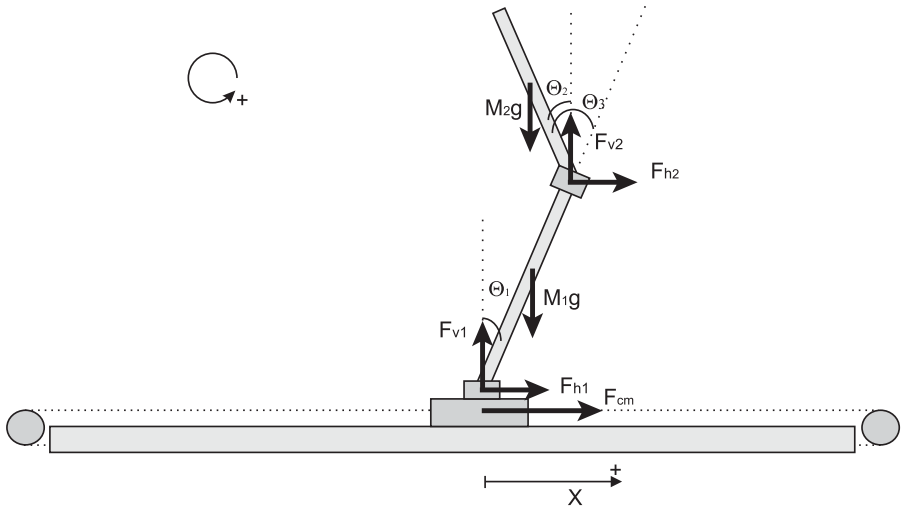

Fig. 12. Principal diagram of the double inverted pendulum system.

The electrical equation:

$$u = K_{tf} U - K_e \dot{\theta}_m - K_{tf} K_{e_{ta}} \dot{\theta}_m,$$

where U is the reference voltage, K_{ft} is a feedback loop filter to control the motor axis speed and the current running into the DC motor is

$$i = \frac{L_a}{R_a} \frac{\mathrm{d}}{\mathrm{d}t} i + \frac{1}{R_a} u.$$

A.2. Pendulum system

The pendulum system consists of the cart and the two aluminum arms.

The dynamics of the cart are given by

$$M_0 \ddot{x} = F_{cm} - F_{H_1}.$$

The dynamics of the two arms are described by three equations for each of them, two equations for the force in the horizontal plane and in the vertical plane and one equation for the torque.

Lower arm:

$$M_1 \frac{\mathrm{d}^2}{\mathrm{d}t^2} \{x + l_{1cm} \sin(\theta_1)\} = F_{H_1} - F_{H_2},$$

$$M_1 \frac{\mathrm{d}^2}{\mathrm{d}t^2} l_{1cm} \cos(\theta_1) = F_{V_1} - F_{V_2} - M_1 g,$$

$$\begin{aligned} I_1 \ddot{\theta}_1 = & -F_{H_1} l_{1cm} \cos(\theta_1) - F_{H_1}(l_1 - l_{1cm}) \cos(\theta_1) \\ & + F_{V_1} l_{1cm} \sin(\theta_1) + F_{V_1}(l_1 - l_{1cm}) \\ & \times \sin(\theta_1) - K_{d_1} M_{d_1}. \end{aligned}$$

Upper arm:

$$M_2 \frac{\mathrm{d}^2}{\mathrm{d}t^2} \{x + l_1 \sin(\theta_1) + l_{2cm} \sin(\theta_2)\} = F_{H_2},$$

$$M_2 \frac{\mathrm{d}^2}{\mathrm{d}t^2} \{l_1 \cos(\theta_1) + l_{2cm} \cos(\theta_2)\} = F_{V_2} - M_2 g,$$

$$I_2 \ddot{\theta}_2 = -F_{H_2} l_{2cm} \cos(\theta_2) + F_{V_2} l_{2cm} \sin(\theta_2) - K_{d_2} M_{d_2}.$$

Parameters for the system are given by

Servo system:

Inertia of the rotor	I_{mr}	$64.7\mathrm{e}^{-7}$ Kgm^2
Rotor inductance	L_a	$65\mathrm{e}^{-6}$ H
Terminal resistance	R_a	0.5 Ω
Motor back EMF—constant	K_e	$21.44\mathrm{e}^{-3}$ $\frac{\mathrm{V}}{\mathrm{rad/s}}$
Torque constant	K_t	$21.44\mathrm{e}^{-3}$ Nm/A
Mass of axle	M_{axle}	0.1 Kg
Mass of cog 1	M_{c_1}	5.3 Kg
Mass of cog 2	M_{c_2}	0.1 Kg
Mass of cog 3	M_{c_3}	0.675 Kg
Radius of axle	r_{axle}	$5\mathrm{e}^{-3}$ m
Radius of cog 1	r_{c_1}	$5.3\mathrm{e}^{-3}$ m
Radius of cog 2	r_{c_2}	$28.27\mathrm{e}^{-3}$ m
Radius of cog 3	r_{c_3}	$30.32\mathrm{e}^{-3}$ m
Gear factor	N	5
Scale constant of the torque disturbance (M_{dm})	K_{dm}	$6.06\mathrm{e}^{-2}$ N
Tacho EMF—constant	$K_{e_{ta}}$	$8.2\mathrm{e}^{-3}$ $\frac{\mathrm{V}}{\mathrm{rad/s}}$

Cart and track:

Mass of cart	M_0	0.81 kg
Length of track	l_t	1.34 m

Lower arm:

Mass of arm	M_1	0.548 kg
Length of arm	l_1	0.535 m
Inertia of arm	I_1	2.678×10^{-2} kg m^2
Length from bottom of arm to center of mass	l_{1cm}	0.355 m
Scaling constant of the torque disturbance M_{d_1}	K_{d_1}	4e^{-4} N
Scaling constant of noise signal n_1	K_{n_1}	1.6e^{-3} N

Upper arm:

Mass of upper arm	M_2	0.21 kg
Length of upper arm	l_2	0.512 m
Inertia of upper arm	I_2	5.217×10^{-3} kg m^2
Length from bottom of arm to center of mass	l_{2cm}	0.12 m
Scaling constant of the torque disturbance M_{d_2}	K_{d_2}	4e^{-4} N
Scaling constant of noise signal n_3	K_{n_3}	1.6e^{-3} N

Appendix B. The system matrices

The system matrices in (2.1) are given in the following.

$$A = \begin{bmatrix} 0 & 1 & 0 & 0 & 0 & 0 & 0 \\ 28.88 & 0 & -3.073 & 0 & 0 & 0 & -3.767 \\ 0 & 0 & 0 & 1 & 0 & 0 & 0 \\ -37.426 & 0 & 34.980 & 0 & 0 & 0 & 0.357 \\ 0 & 0 & 0 & 0 & 0 & 1 & 0 \\ -3.211 & 0 & 0.025 & 0 & 0 & 0 & 1.899 \\ 0 & 0 & 0 & 0 & 0 & -1.305 \times 10^6 & -7.692 \times 10^3 \end{bmatrix},$$

$$B_w = \begin{bmatrix} 0 & 0 & 0 & 0 & 0 & 0 & 0 \\ 0 & 0.004 & -0.005 & 0 & 0 & 10.656 & 0 \\ 0 & 0 & 0 & 0 & 0 & 0 & 0 \\ 0 & -0.005 & -0.057 & 0 & 0 & -1.010 & 0 \\ 0 & 0 & 0 & 0 & 0 & 0 & 0 \\ 0 & -0.004 & 0 & 0 & 0 & -5.370 & 0 \\ 0 & 0 & 0 & 0 & 0 & 0 & 0 \end{bmatrix},$$

$$B_u = \begin{bmatrix} 0 \\ 0 \\ 0 \\ 0 \\ 0 \\ 0 \\ 1.045 \times 10^6 \end{bmatrix},$$

$$C_z = \begin{bmatrix} 0 & 0 & 0 & 0 & -1 & 0 & 0 \\ 1 & 0 & 0 & 0 & 0 & 0 & 0 \\ 0 & 0 & 1 & 0 & 0 & 0 & 0 \\ 0 & 0 & 0 & 0 & 0 & 0 & 0 \\ 0 & 0 & 0 & 0 & 0 & 0 & 1 \end{bmatrix},$$

$$D_{zw} = \begin{bmatrix} 1 & 0 & 0 & 0 & 0 & 0 & -5.0 \times 10^{-4} \\ 0 & 0 & 0 & 1.6 \times 10^{-3} & 0 & 0 & 0 \\ 0 & 0 & 0 & 0 & 1.6 \times 10^{-3} & 0 & 0 \\ 0 & 0 & 0 & 0 & 0 & 0 & 0 \\ 0 & 0 & 0 & 0 & 0 & 0 & 0 \end{bmatrix},$$

$$D_{zu} = \begin{bmatrix} 0 \\ 0 \\ 0 \\ 1 \\ 0 \end{bmatrix},$$

$$C_y = \begin{bmatrix} 0 & 0 & 0 & 0 & -1 & 0 & 0 \\ 1 & 0 & 0 & 0 & 0 & 0 & 0 \\ -1 & 0 & 1 & 0 & 0 & 0 & 0 \end{bmatrix},$$

$$D_{yw} = \begin{bmatrix} 1 & 0 & 0 & 0 & 0 & 0 & -5.0 \times 10^{-4} \\ 0 & 0 & 0 & 1.6 \times 10^{-3} & 0 & 0 & 0 \\ 0 & 0 & 0 & 0 & 1.6 \times 10^{-3} & 0 & 0 \end{bmatrix},$$

$$D_{yu} = \begin{bmatrix} 0 \\ 0 \\ 0 \end{bmatrix}.$$

Appendix C. The controller gains

$$F^T = \begin{bmatrix} 9.1927 \times 10^{-1} \\ -1.6179 \times 10^{-1} \\ -2.6540 \\ -4.4355 \times 10^{-1} \\ -1.1004 \times 10^{-1} \\ 9.3996 \times 10^{-1} \\ 6.6792 \times 10^{-3} \end{bmatrix},$$

$$L = \begin{bmatrix} -6.5974 & -3.5155 & -2.5714 \times 10^{2} \\ 1.5959 \times 10^{3} & 2.7918 \times 10^{4} & 1.1242 \times 10^{5} \\ -1.0141 \times 10^{-1} & 3.2692 \times 10^{1} & 5.4001 \times 10^{1} \\ -1.5316 \times 10^{2} & -2.5707 \times 10^{3} & -1.0625 \times 10^{4} \\ 4.0120 \times 10^{1} & -1.9870 \times 10^{3} & -1.7220 \times 10^{3} \\ -8.1819 \times 10^{2} & -1.3322 \times 10^{4} & -5.5947 \times 10^{4} \\ 1.5908 \times 10^{5} & 2.4278 \times 10^{6} & 9.9745 \times 10^{6} \end{bmatrix},$$

$$Q_{nom} = [1.0426 \times 10^{-2} \;\; 3.6693 \times 10^{-2} \;\; 2.9514 \times 10^{-2}].$$

References

Alazard, D., & Apkarian, P. (1999). Exact observer-based structures for arbitrary compensators. *International Journal of Robust and Nonlinear Control*, *9*, 101–118.

Alazard, D., & Apkarian, P. (2002). Matlab package for calculation of observer based controller structure. Available at: http://www.su-paero.fr/page-perso/autom/alazard/demos/demo_obr.html.

Blanke, M., Frei, C. W., Kraus, F., Patton, R. J., & Staroswiecki, M. (2000). What is fault-tolerant control? In *Preprints of fourth IFAC symposium on fault detection supervision ans safety for technical processes*, *SAFEPROCESS'2000*, Budapest, Hungary (pp. 40–51).

Blanke, M., Staroswiecki, M., & Wu, E. (2001). Concepts and methods in fault-tolerant control. In *Proceedings of American control conference*, *ACC-2001*, Washington DC, USA (pp. 2606–2620).

Frank, P. M., & Ding, X. (1994). Frequency domain approach to optimally robust residual generation and evaluation for model-based fault diagnosis. *Automatica*, *30*, 789–804.

Gertler, J. (1998). *Fault detection and diagnosis in engineering systems*. New York: Marcel Dekker.

Kucera, V. (1975). Stability of discrete linear feedback systems. In *Proceedings of the sixth IFAC world congress*, Boston, MA, Paper 44.1.

Niemann, H., & Poulsen, J. K. (2003). Analysis and design of controllers for a double inverted pendulum. In *Proceedings of the American control conference*, Denver, CO, USA (pp. 2903–2808).

Niemann, H. H., & Poulsen, J. K. (2005). Design and analysis of controllers for an inverted double pendulum. *ISA Transactions*, to appear.

Niemann, H., & Stoustrup, J. (2002). Reliable control using the primary and dual Youla parameterization. *In Proceedings of the 41st IEEE conference on decision and control*, Las Vegas, NV, USA (pp. 4353–4358).

Niemann, H. H., & Stoustrup, J. (2004). Fault tolerant controllers for sampled-data systems. In *Proceedings of the American control conference*, Boston, MA, USA (pp. 3490–3495).

Niemann, H. H., Stoustrup, J., & Abrahamsen, R. B. (2004). Switching between multivariable controllers. *Optimal control–application and methods* (pp. 51–66).

Poulsen, J. K. (2001). Modelling and control of unstable system. Master's thesis. Automation, Ørsted-DTU, Technical University of Denmark, DK-2800 Lyngby, Denmark.

Skogestad, S., & Postlethwaite, I. (1996). *Multivariable feedback control—Analysis and design*. New York: Wiley.

Stoustrup, J., & Niemann, H. H. (2001). Fault tolerant feedback control using the youla parameterization. In *Proceedings of the sixth European control conference*, Porto, Portugal (p. 6).

Tay, T. T., Mareels, I. M. Y., & Moore, J. B. (1997). *High performance control*. Basel: Birkhäuser.

Wu, N. E., & Chen, T. J. (1996). Feedback design in control reconfigurable systems. *International Journal of Robust and Nonlinear Control*, *6*(6), 561–570.

Wu, N. E., Zhou, K., & Salomon, G. (2000). Control reconfigurability of linear time-invariant systems. *Automatica*, *36*, 1767–1771.

Youla, D. C., Bongiorno, J. J., & Jabr, H. A. (1976a). Modern Wiener–Hopf design of optimal controllers—Part I: The single-input-output case. *IEEE Transactions on Automatic Control*, *21*(1), 3–13.

Youla, D. C., Jabr, J. J., & Bongiorno, H. A. (1976b). Modern Wiener–Hopf design of optimal controllers—Part II: The multivariable case. *IEEE Transactions on Automatic Control*, *21*(3), 319–338.

Zhou, K., & Ren, Z. (2001). A new controller architecture for high performance robust, and fault-tolerant control. *IEEE Transactions on Automatic Control*, *46*(10), 1613–1618.

Zhou, K., Doyle, J. C., & Glover, K. (1995). *Robust and optimal control*. New York: Prentice-Hall.